

# Electronic and Vibrational Spectroscopic Investigation of Phenylacetylene–Amine Complexes. Evidence for the Diversity in the Intermolecular Structures

Prashant Chandra Singh and G. Naresh Patwari\*

Department of Chemistry, Indian Institute of Technology Bombay, Powai, Mumbai 400076, India

Received: January 4, 2008; Revised Manuscript Received: February 25, 2008

Shifts in the electronic transitions for the complexes of phenylacetylene with ammonia, methylamine, and triethylamine clearly indicate the variation in the intermolecular structures of the three complexes. The infrared spectrum of phenylacetylene in the acetylenic C–H stretching region shows Fermi resonance bands, which act as a sensitive tool to probe the intermolecular structures. The IR-UV double resonance spectra of the three complexes are disparate and signify the formation of distinct structures. The formation of C–H···N hydrogen-bonded complex with ammonia and two distinct types of  $\pi$  complexes with methylamine and triethylamine can be inferred from the analysis of electronic and vibrational spectra in combination with *ab initio* calculations. These complexes clearly point out the fact that marginal changes in the interacting partner can significantly alter the intermolecular structure.

## Introduction

Phenylacetylene is an interesting molecule to investigate competitive hydrogen bonding as it has two hydrogen bond acceptor groups in the form of  $\pi$  electron densities of the benzene ring and an acetylenic C $\equiv$ C bond. On the other hand, the relatively acidic acetylenic C–H group can also act as a hydrogen bond donor. It is now well-established that in the case of the benzene–ammonia complex the N–H group of ammonia interacts with  $\pi$  electron density of the benzene ring, resulting in the formation of a N–H··· $\pi$  hydrogen bond,<sup>1</sup> whereas the acetylene–ammonia complex is characterized by a linear C–H···N “ $\sigma$ ” hydrogen bond.<sup>2</sup> The structure of the phenylacetylene–ammonia complex will be an outcome of the balance of energies between the two sets of interactions. Castleman’s group has reported the REMPI and ion-dip spectra of the phenylacetylene–ammonia complex.<sup>3,4</sup> On the basis of the shift in the origin band of the complex in the REMPI spectrum and in comparison with complexes of ammonia with benzene<sup>5</sup> and phenol,<sup>6</sup> it was proposed that the ammonia is located between the benzene ring and the C $\equiv$ C bond region of phenylacetylene. However, no conclusive experimental proof was offered to substantiate such an assignment. In the light of these observations, we have carried out vibrational spectroscopic investigation using a IR-UV double resonance spectroscopic technique to determine the structure of the phenylacetylene–ammonia complex. Further, we have also investigated the complexes of phenylacetylene with methylamine and triethylamine. The rationale for such an investigation was two fold: first, to understand the effect of increased basicity and second, to understand the effect of methyl group substitution on the intermolecular structure and the energetics.

## Experimental and Theoretical Methods

Helium buffer gas at 4 atm is bubbled through a mixture of phenylacetylene (Aldrich) and amines kept at room temperature and expanded through a 0.5 mm diameter pulsed nozzle (Series 9, Iota One; General Valve Corporation). The electronic

excitation of phenylacetylene and its amine clusters was achieved using a frequency doubled output of a tunable dye laser (Narrow Scan GR; Radiant Dyes; operating with Rhodamine-19 dye) pumped with the second harmonic of a Nd:YAG laser (Surelite I-10; Continuum). For the phenylacetylene monomer and its ammonia complex, one color resonant two photon ionization (1C-R2PI) technique was used, whereas a laser induced fluorescence (LIF) technique was used for complexes of phenylacetylene with methylamine and triethylamine, to observe the electronic excitation spectra. The LIF spectrum was recorded by monitoring the total fluorescence with a photomultiplier tube (9780SB + 1252–5F; Electron Tubes Limited) and a filter (BG3 + WG-305) combination, and the 1C-R2PI spectra were recorded by monitoring the appropriate mass signal with a time-of-flight mass spectrometer using a channeltron (KBL-25RS; Sjets) detector, while scanning UV laser frequency. The choice of either 1C-R2PI or LIF was based on obtaining a better S/N ratio. The IR spectra were obtained either using fluorescence dip infrared (FDIR) or ion dip infrared (IDIR) spectroscopic methods. In our experiments the source of tunable IR light was an idler component of a LiNbO<sub>3</sub> OPO (Custom IR OPO; Euroscan Instruments) pumped with an injection seeded Nd:YAG laser (Brilliant-B; Quantel).<sup>7</sup> The typical bandwidth of both the UV and IR lasers is about 1 cm<sup>–1</sup>. The energy obtained by IR OPO was typically about  $\sim$ 2 mJ/pulse in the range scanned, with an exception of the  $\sim$ 3450–3490 cm<sup>–1</sup> region where the OPO oscillation diminishes due to an intense IR absorption of the LiNbO<sub>3</sub> crystal. Therefore, the transitions in the N–H stretching region could not be probed.

To get further insights into experimental results, *ab initio* calculations were carried out using the Gaussian-03 suit of programs.<sup>8</sup> The equilibrium structures of the monomers and various complexes were calculated at the MP2(FC)/aug-cc-pVDZ level of theory for the ammonia and methylamine complexes. The nature of the stationary points obtained were verified by calculating the vibrational frequencies at the same level of theory. The calculated vibrational frequencies were scaled for the monomers to match with the experimental values, and the same scaling factor was used for the corresponding complexes. The stabilization energies were calculated and in

\* E-mail: naresh@chem.iitb.ac.in.

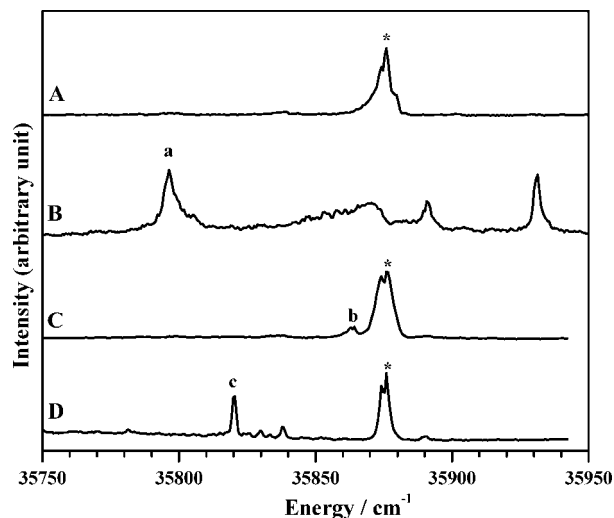


**Figure 1.** 1C-R2PI spectra of phenylacetylene (trace A) and phenylacetylene–ammonia complex (trace B). LIF spectra of phenylacetylene–methylamine (trace C) and phenylacetylene–triethylamine (trace D) complexes. The peaks marked with “\*” are band-origin transition of the phenylacetylene monomer, whereas those marked with “a”, “b”, and “c” are the band-origin transitions for the ammonia, methylamine, and triethylamine complexes, respectively.

each case were corrected for the zero point vibrational energy (ZPVE) and 50% basis set superposition error (BSSE). According to Kim et al., 100% of BSSE correction often underestimates the interaction energy, and 50% correction is a good empirical approximation; therefore, 50% BSSE corrected binding energies are reported here.<sup>9</sup>

## Results and Discussion

Figure 1A shows one color resonant two photon ionization (1C-R2PI) spectrum of phenylacetylene, recorded by monitoring the 102 amu peak. In this spectrum the intense peak at 35 876  $\text{cm}^{-1}$ , marked with an asterisk, corresponds to band-origin of the  $S_1 \leftarrow S_0$  transition, which is in good agreement with the value reported in the literature.<sup>10</sup> Figure 1B shows the 1C-R2PI excitation spectrum of the phenylacetylene–ammonia complex, recorded by mass gating at 119 amu, corresponding to the binary cluster. This spectrum shows several transitions, and the transition at 35 796  $\text{cm}^{-1}$ , marked “a”, is the origin band of the binary complex, which is in good agreement with that reported by Castleman’s group.<sup>3</sup> This band-origin transition of the phenylacetylene–ammonia complex is shifted by  $-80 \text{ cm}^{-1}$  relative to the bare phenylacetylene. Further, the transition at 35 890  $\text{cm}^{-1}$  ( $+14 \text{ cm}^{-1}$ , relative to bare phenylacetylene) was also assigned to the band origin of an isomeric structure, whereas transition at 35 931  $\text{cm}^{-1}$  ( $+55 \text{ cm}^{-1}$ ) was assigned to a vibronic band.<sup>3</sup> In the present spectrum the broad transition peaking around 35 870  $\text{cm}^{-1}$  can be assigned to that arising out of fragmentation of the higher complexes of ammonia and leading to the formation of binary complex. The LIF spectra of phenylacetylene in the presence of methylamine and triethylamine are depicted in Figure 1, panels C and D, respectively. The transition at 35 864  $\text{cm}^{-1}$ , marked “b”, in Figure 1C and the transition at 35 820  $\text{cm}^{-1}$ , marked “c”, in Figure 1D are the band origin transitions of methylamine and triethylamine complexes, respectively. The band origin transitions of the phenylacetylene complexes with ammonia, methylamine, and triethylamine are shifted by  $-80$ ,  $-12$ , and  $-56 \text{ cm}^{-1}$ , respectively, relative to the bare phenylacetylene. The trend in the gas phase proton affinities of ammonia, methylamine, and

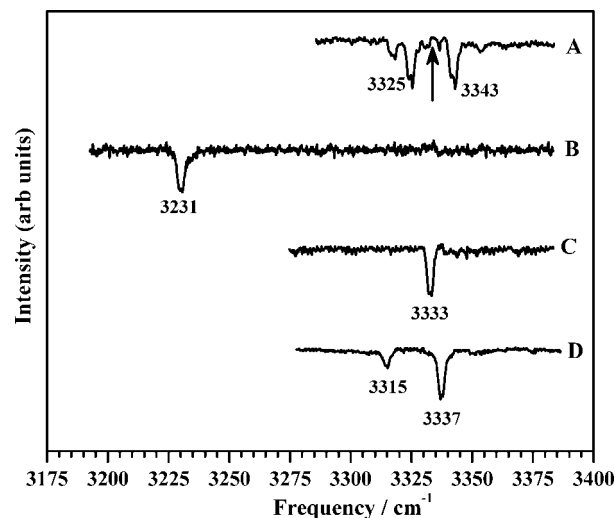


**Figure 2.** IDIR spectra of phenylacetylene (trace A) and the phenylacetylene–ammonia complex (trace B). FDIR spectra of phenylacetylene–methylamine (trace C) and phenylacetylene–triethylamine (trace D) complexes. The arrow in trace A indicates the position of the unperturbed acetylenic C–H stretching frequency at 3334  $\text{cm}^{-1}$ .

triethylamine are in increasing order. If the structures of all the three complexes are similar, then a correlation between the shifts in the band origin transitions and proton affinities is expected, similar that observed in the case of phenol complexes.<sup>11</sup> However, no such correlation can be obtained for the present three complexes, which strongly indicates that the binding modes of phenylacetylene with ammonia and the two amines are different.

Figure 2A depicts the IDIR spectrum of bare phenylacetylene, which shows several transitions. Sterns and Zwier have assigned the two strong transitions at 3325 and 3343  $\text{cm}^{-1}$  to the Fermi resonance bands between C–H stretching vibration and a combination of one quantum of  $\text{C}\equiv\text{C}$  stretch and two quanta of  $\text{C}\equiv\text{C}$ –H out-of-plane bend and other weak features to the transitions arising out of higher order coupling terms.<sup>12</sup> The stretching frequency of an unperturbed acetylenic C–H group can be estimated as 3334  $\text{cm}^{-1}$  using the deperturbation analysis.<sup>13,14</sup> The IDIR spectrum of the phenylacetylene–ammonia complex depicted in Figure 2B shows a single transition at 3231  $\text{cm}^{-1}$ , which can be assigned to the acetylenic C–H stretching vibration of the complex. The C–H stretching vibration of the complex shows a substantial shift of 103  $\text{cm}^{-1}$  to a lower frequency relative to the phenylacetylene monomer, which clearly indicates the formation of  $\text{C}-\text{H}\cdots\text{N}$  “ $\sigma$ ” hydrogen-bonded complex between phenylacetylene and ammonia. The strong interaction between the acetylenic C–H group and the ammonia perturbs the Fermi resonance condition, thereby leading to a single transition.

The FDIR spectrum of the methylamine complex, depicted in Figure 2C, surprisingly shows a single transition at 3333  $\text{cm}^{-1}$ . The lone transition can be assigned to the C–H stretching vibration of the phenylacetylene–methylamine complex, which is shifted to a lower frequency by 1  $\text{cm}^{-1}$ , relative to the bare phenylacetylene.<sup>14</sup> Further, this spectrum indicates that the methylamine is interacting with the acetylenic moiety of phenylacetylene, thereby perturbing the Fermi resonance condition, which leads to appearance of a single transition. Because the shift in the C–H stretching vibration is very marginal, it can be expected that the N–H group of methylamine interacting with  $\pi$  electron density of either the benzene ring or the

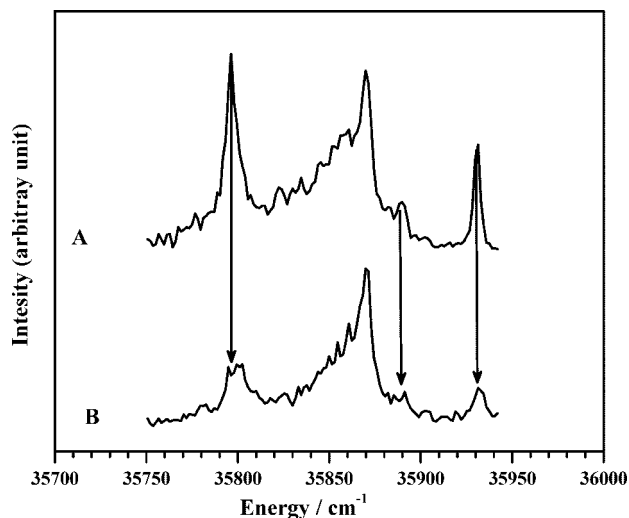


**Figure 3.** 1C-R2PI spectrum of the phenylacetylene–ammonia complex (trace A) and the IR-UV hole-burnt spectrum of the phenylacetylene–ammonia complex, which was recorded by pumping the C–H stretching vibration of the complex with an IR laser fixed at  $3231\text{ cm}^{-1}$  prior to the ionizing (1C-R2PI) UV laser (trace B). The arrows point the bands with reduced intensities in the hole-burnt spectrum.

acetylenic  $\text{C}\equiv\text{C}$  bond or both. Figure 2D depicts the FDIR spectrum of the triethylamine complex, which shows two transitions at  $3315$  and  $3337\text{ cm}^{-1}$ . Prima-facie it appears that the interaction of triethylamine with phenylacetylene marginally alters the zero-order (unperturbed) frequencies and the coupling, which leads to minor changes in the frequencies of the observed bands and redistribution of intensities of the Fermi resonance bands. This situation is very much unlike the interaction of phenylacetylene with ammonia and methylamine. One would expect such a situation in the event of triethylamine interacting exclusively with the benzene  $\pi$  electron density. The IR spectra clearly signify that the mode of binding of the three solvent molecules with phenylacetylene is different.

Breen et al. had earlier reported the R2PI spectrum of the phenylacetylene–ammonia complex, wherein the bands shifted by  $-80$  and  $+14\text{ cm}^{-1}$ , relative to the band-origin of bare phenylacetylene at  $35\,876\text{ cm}^{-1}$ , were assigned to be originating from two different isomers.<sup>3</sup> However, hole-burning spectroscopy was not carried out to substantiate these assignments. We have carried out IR-UV hole burning spectroscopy to investigate the origin of these two bands and the results are presented in the Figure 3. Trace A, shows the 1C-R2PI spectrum of the phenylacetylene–ammonia complex. Trace B is the IR-UV hole-burnt spectrum, which was recorded by tuning the IR laser to pump the C–H vibrational transition at  $3231\text{ cm}^{-1}$  (see Figure 2B),  $50\text{ ns}$  prior to the R2PI–UV pulse, while scanning the UV laser. The hole-burnt spectrum shows diminished intensities for all three bands appearing at  $-80$ ,  $+14$ , and  $+55\text{ cm}^{-1}$ , which implies that all the three observed bands in the R2PI spectrum are originating from a single isomer. The present results, both in terms of number of isomers and the mode of interaction, are completely in contrast to the observations made by Breene et al.<sup>3</sup>

To supplement the experimental observations and to enhance the understanding of modes of intermolecular interaction, ab initio calculations were carried out. The complexes of ammonia and methylamine were investigated at the MP2/aug-cc-pVDZ level. However, due to limitation in our computational resources, the triethylamine complex was left out. For the complexes of

phenylacetylene with ammonia and methylamine, the calculations were carried out using about a dozen variants in the initial geometries in each case. However, only three true minima were identified on both the cases. The optimized structures of the binary complexes of phenylacetylene with ammonia and methylamine are shown in Figure 4. The first phenylacetylene–ammonia complex is a linear  $\text{C}-\text{H}\cdots\text{N}$   $\sigma$  hydrogen-bonded complex (Figure 4A) wherein the acetylenic C–H group of phenylacetylene is a hydrogen bond donor to the lone pair on ammonia. The second structure (Figure 4B) is a  $\text{N}-\text{H}\cdots\pi$  hydrogen-bonded complex, wherein the benzene ring of the phenylacetylene moiety acts as hydrogen bond acceptor. The third complex (Figure 4C) is a quasiplanar cyclic structure with both phenylacetylene and ammonia acting as donors and acceptors. In this case the N–H group of the ammonia moiety is interacting with the acetylenic  $\text{C}\equiv\text{C}$  bond, and the lone pair of ammonia is interacting with the benzene C–H group in the ortho position. Methylamine also yields a linear  $\text{C}-\text{H}\cdots\text{N}$   $\sigma$  hydrogen-bonded complex, depicted in Figure 4D. The second complex of methylamine is a  $\text{N}-\text{H}\cdots\pi$  hydrogen-bonded complex with a peripheral interaction between the methyl C–H group and the acetylenic  $\text{C}\equiv\text{C}$  bond (Figure 4E). The third complex has a cyclic structure (Figure 4F), wherein the N–H group of methylamine interacts with the acetylenic  $\text{C}\equiv\text{C}$  bond and the C–H group of benzene in the ortho position is interacting with the nitrogen lone-pair. The structure of this complex is very similar to the cyclic ammonia complex (Figure 4C), but with the methyl group pointing out of the plane. The binding energies, listed in Table 1, indicate that the  $\text{C}-\text{H}\cdots\text{N}$   $\sigma$  hydrogen-bonded ammonia complex (Figure 4A) is marginally more stable than the other two isomers. In the case of methylamine, the  $\text{N}-\text{H}\cdots\pi$  hydrogen-bonded complex (Figure 4E) is relatively more stable, which is in sharp contrast with the ammonia complex.

Infrared spectroscopy has been a major tool to investigate the structure and dynamics of hydrogen-bonded complexes, especially in the hydride ( $\text{X}-\text{H}$ ;  $\text{X} = \text{O}, \text{N}, \text{C}$ ) stretching region. This is due to the fact that these stretching frequencies are very sensitive to hydrogen-bonded structures, because they are directly involved in the hydrogen bond formation and show a characteristic shift to a lower frequency upon hydrogen bonding.<sup>15</sup> On the basis of the shifts in the vibrational transitions one can assign the possible intermolecular structure of the complex. Table 1 also lists the calculated vibrational frequencies that were scaled by a factor of  $0.958$  so as to match the unperturbed experimental acetylenic C–H frequency of the phenylacetylene monomer, and the same scaling factor was used throughout. The  $\text{C}-\text{H}\cdots\text{N}$   $\sigma$  hydrogen-bonded complexes of both ammonia and methylamine show a very large shift (in excess of  $100\text{ cm}^{-1}$ ) towards lower frequency in the acetylenic C–H stretching vibration. However, only the IR spectrum of the ammonia complex (Figure 2B) shows a substantial ( $103\text{ cm}^{-1}$ ) shift in the C–H stretching frequency, which is in good agreement with the calculated shift of  $134\text{ cm}^{-1}$ . Therefore, the ammonia complex can be unambiguously assigned to the linear  $\text{C}-\text{H}\cdots\text{N}$  “ $\sigma$ ” hydrogen-bonded complex. This assignment is in complete contrast with the structure proposed by Breene et al. wherein the ammonia is located between the benzene ring and the acetylenic  $\text{C}\equiv\text{C}$  bond region.<sup>3</sup>

On the basis of the observed IR spectrum for the methylamine complex (Figure 2C) the  $\text{C}-\text{H}\cdots\text{N}$   $\sigma$  hydrogen-bonded complex can be completely ruled out. The most important and interesting feature of the FDIR spectrum of the phenylacetylene–methylamine complex is the disappearance of Fermi resonance

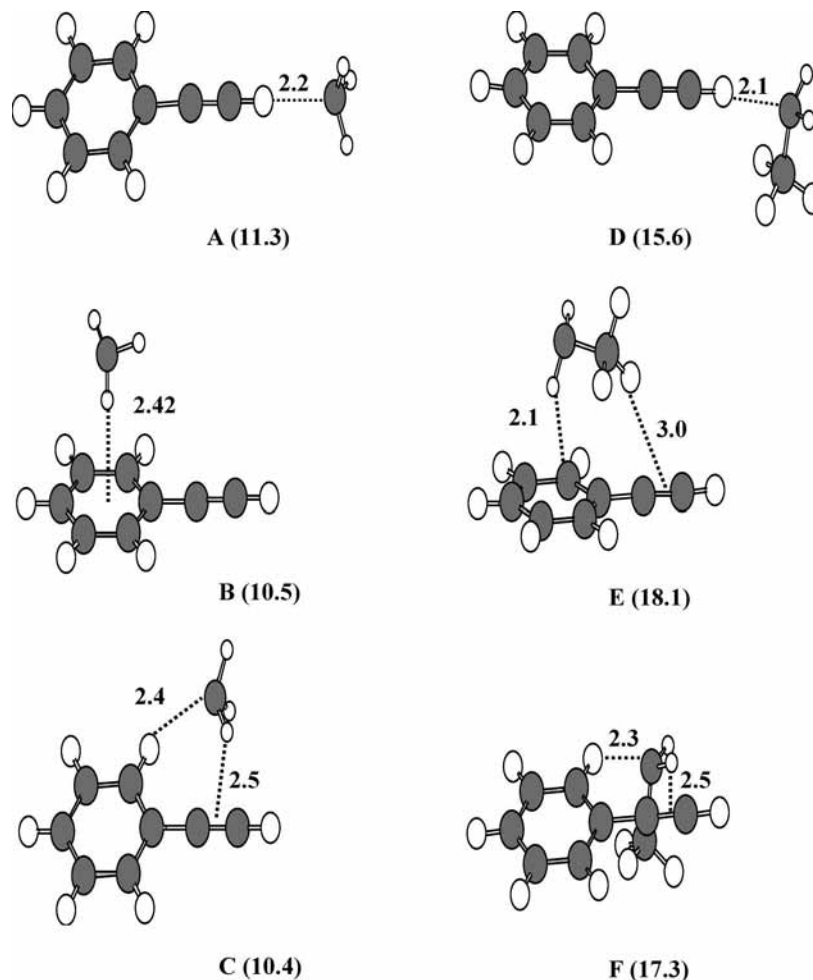


**Figure 4.** Calculated structures of phenylacetylene complexes with ammonia (A–C) and methylamine (D–F) at the MP2/aug-cc-pVDZ level. The distances are shown in Å, and the binding energy ( $\text{kJ mol}^{-1}$ ) for each complex is given in parenthesis.

**TABLE 1: Binding Energies ( $\text{kJ mol}^{-1}$ ), Scaled Vibrational Frequencies ( $\text{cm}^{-1}$ ), and Their Shifts for the Phenylacetylene Complexes with Ammonia and Methylamine Calculated at the MP2/aug-cc-pVDZ Level of Theory**

	$\Delta E$	$\nu_{\text{C-H}}$	$\Delta\nu_{\text{C-H}}$	$\nu_{\text{N-H}}^a$	$\Delta\nu_{\text{N-H}}$
PHA		3334			
$\text{NH}_3$				3484 (as), 3335 (s)	
$\text{NH}_2\text{Me}$				3458 (as), 3364 (s)	
PHA- $\text{NH}_3$ (A)	11.3	3200	-134	3474 (as), 3328 (s)	-10, -7
PHA- $\text{NH}_3$ (B)	10.5	3330	-4	3463 (hb), 3318 (f)	-21, -17
PHA- $\text{NH}_3$ (C)	10.4	3332	-2	3469 (hb), 3325 (f)	-15, -10
PHA- $\text{NH}_2\text{Me}$ (D)	15.6	3163	-171	3453 (as), 3360 (s)	-5, -4
PHA- $\text{NH}_2\text{Me}$ (E)	18.1	3332	-2	3447 (hb), 3355 (f)	-11, -9
PHA- $\text{NH}_2\text{Me}$ (F)	17.3	3330	-4	3448 (hb), 3351 (f)	-10, -13

<sup>a</sup> For the O–H vibrations “s”, “as”, “hb”, and “f” indicate symmetric, anti-symmetric, hydrogen-bonded, and free stretching frequencies, respectively.

bands in the acetylenic C–H region, leading to a single transition. Because the Fermi resonance in the phenylacetylene monomer involves a C–H stretching vibration and a combination of one quantum of  $\text{C}\equiv\text{C}$  stretch and two quanta of  $\text{C}\equiv\text{C-H}$  out-of-plane bend, the disappearance of the Fermi resonance indicates that methylamine is either interacting with the C–H oscillator or the  $\text{C}\equiv\text{C}$  oscillator or both. The FDIR spectrum of the methylamine complex rules out the possibility of interacting with the C–H oscillator, therefore the disappearance of the Fermi resonance can be attributed to the interaction of methylamine with the  $\pi$  electron density of the acetylenic  $\text{C}\equiv\text{C}$  bond. Both

structures shown in Figure 4, panels E and F, account for such an interaction. However, the binding energies clearly indicates that the  $\text{N-H}\cdots\pi$  hydrogen-bonded complex with a peripheral interaction between the methyl C–H group and the acetylenic  $\text{C}\equiv\text{C}$  bond (Figure 4E) is marginally favored ( $0.8 \text{ kJ mol}^{-1}$ ) over the cyclic complex (Figure 4F). The IR spectrum of the phenylacetylene–methylamine complex is almost identical similar to the phenylacetylene–water complex, which has cyclic structure similar to 4F.<sup>16</sup> However, the shift in the electronic transitions of the two complexes are quite opposite in nature. In the case of methylamine complex, the electronic transition is shifted by  $-12 \text{ cm}^{-1}$ , whereas in the case of water the corresponding transition is shifted by  $+14 \text{ cm}^{-1}$ .<sup>16</sup> Comparison with the water cluster and the higher binding energy clearly supports the formation of a  $\text{N-H}\cdots\pi$  hydrogen-bonded phenylacetylene–methylamine complex, shown in Figure 4E.

The FDIR spectrum of the triethylamine complex (Figure 2D) clearly shows the presence of Fermi resonance, albeit with some intensity redistribution. The observed peak positions once again clearly rule out the possibility of a linear  $\text{C-H}\cdots\text{N}$   $\sigma$  hydrogen-bonded complex. Further, the presence of Fermi resonance bands also indicates the absence of interaction with the  $\pi$  electron density of the acetylenic  $\text{C}\equiv\text{C}$  bond. Additionally, the shift in the origin band of the electronic transition of triethylamine complex ( $-56 \text{ cm}^{-1}$ ) is lower than ammonia complex ( $-80 \text{ cm}^{-1}$ ), is higher than the methylamine complex ( $-12 \text{ cm}^{-1}$ ), and is comparable to the argon complex ( $-30 \text{ cm}^{-1}$ ).<sup>10</sup> On the basis of the shift in the electronic transition and the observed



structure in the FDIR spectrum, the triethylamine can be envisaged to be bound to the benzene  $\pi$  electron density of phenylacetylene, predominantly through dispersion interaction.

The absence of IR spectra in the N–H stretching region for the ammonia and methylamine complexes are perhaps the missing pieces of evidence in the assignment of the intermolecular structures. However, it can be argued that the large shift in the acetylenic C–H stretching frequency in the ammonia complex can only be attributed to the formation of the linear C–H $\cdots$ N  $\sigma$  hydrogen-bonded complex, and thus the assignment is unambiguous. In the case of the methylamine complex, the marginal shift of 1  $\text{cm}^{-1}$  in the acetylenic C–H stretching frequency unambiguously rules out the possibility of a linear C–H $\cdots$ N  $\sigma$  hydrogen-bonded complex. For the remaining two structures (Figure 4, panels E and F) the differences in the frequencies of the N–H stretching vibrations are very marginal (see Table 1). Therefore, one would fall back on the arguments used earlier to arrive at the intermolecular structure. This, however, does not completely justify the absence of the IR spectra in the N–H stretching region, which could not be obtained due to the hole in the tuning range of our OPO in the  $\sim$ 3450–3490  $\text{cm}^{-1}$  region. On the other hand, the Fermi resonance bands, their appearance and disappearance, are sensitive enough to probe the nature of intermolecular interaction in the phenylacetylene complexes, which in the present case, and along with the shifts in the electronic transitions, make up for the lack of spectra in the N–H stretching region.

The infrared spectrum of the phenylacetylene–ammonia complex (Figure 2B) in the acetylenic C–H stretching frequency shows a red shift of 103  $\text{cm}^{-1}$ , relative to bare phenylacetylene. This clearly and unambiguously illustrates the formation of a linear C–H $\cdots$ N  $\sigma$  hydrogen-bonded complex. The substitution of alkyl groups on ammonia increases the basicity, which in turn is expected to enhance the  $\sigma$  hydrogen-bonded interaction. For instance, in the case of hydrogen-bonded complexes of phenol, the lowering of the O–H stretching frequency increases with the increase in basicity of the interacting amine.<sup>17</sup> A similar consideration for the hydrogen-bonded complexes of phenylacetylene would indicate that the acetylenic C–H stretching frequency should be further lowered when interacting with methylamine and triethylamine, relative to the ammonia complex. However, the observed shifts in the C–H stretching frequency for the methylamine (Figure 2C) and triethylamine (Figure 2D) complexes are marginal and rule out the formation of C–H $\cdots$ N  $\sigma$  hydrogen-bonded complexes. Substitution by a single methyl group on ammonia leads to formation of a N–H $\cdots$  $\pi$  (benzene  $\pi$ ) hydrogen-bonded complex, which is indicative of substantial change in the binding mode relative to ammonia. The analysis of spectral shifts both in the electronic and vibrational transitions in combination with the ab-initio calculations also suggest the involvement of secondary interaction in the form of C–H $\cdots$  $\pi$  (acetylene  $\pi$ ) hydrogen bond. In the case of the ammonia complex, the electrostatic contribution to the binding energy dominates leading to the formation of a C–H $\cdots$ N  $\sigma$  hydrogen bond. On the other hand, in the case of the methylamine complex, both the N–H $\cdots$  $\pi$  and the C–H $\cdots$  $\pi$  interactions, which are primarily dispersive in nature, dominate. The change in the intermolecular structure is perhaps due to the domination of the two dispersive interactions in the methylamine complex, which cooperatively stabilize each other, over the electrostatic interaction. The trend continues with the triethylamine complex in which dispersive interactions completely take over. The hydrogen bonding in phenylacetylene can be viewed as a subtle balance between the electrostatic and

dispersion forces, unlike the case of phenol wherein electrostatic forces dominate.

## Conclusions

The shifts in the electronic transitions of the phenylacetylene complexes with ammonia ( $-80 \text{ cm}^{-1}$ ), methylamine ( $-12 \text{ cm}^{-1}$ ), and triethylamine ( $-56 \text{ cm}^{-1}$ ), which lack in any trend, are the primary indication of variation in the intermolecular structure of these three complexes. A large shift of 103  $\text{cm}^{-1}$  to a lower frequency in the acetylenic C–H stretching vibration in the ammonia complex provides an unambiguous evidence for the formation of the linear C–H $\cdots$ N  $\sigma$  hydrogen-bonded complex. This structure of the ammonia complex is in contradiction to that reported earlier in the literature. Small shifts in the electronic transition accompanied by disappearance of Fermi resonance bands substantiate the formation of N–H $\cdots$  $\pi$  hydrogen-bonded complex with methylamine, which accompanies a peripheral interaction of methyl C–H with the acetylenic C $\equiv$ C bond. The triethylamine binds to the  $\pi$  electron cloud of benzene ring primarily through dispersion interactions. The redistribution of intensities in the Fermi resonance bands supports formation of such a structure. The basicity of ammonia, methylamine, and triethylamine increases in that order; however, the formation of C–H $\cdots$ N hydrogen-bonded complexes is not favored. These present complexes clearly demonstrate that the intermolecular structure can drastically change by replacing a single hydrogen atom with a methyl group.

**Acknowledgment.** This material is based upon work supported by Department of Science and Technology (Grant No. SR/S1/PC-40/2003), Board of Research in Nuclear Sciences (Grant No. 2004/37/5/BRNS/398), and Council of Industrial and Scientific Research (Grant No. 01(1902)/03/EMR-II). P. C. S. thanks CSIR for the award of senior research fellowship.

## References and Notes

- (1) Rodham, D. A.; Suzuki, S.; Suenram, R. D.; Lovas, F. J.; Dasgupta, S.; Goddard, W. A.; Blake, G. A. *Nature* **1993**, *362*, 735.
- (2) Fraser, G. T.; Leopold, K. R.; Klemperer, W. *J. Chem. Phys.* **1984**, *80*, 1423.
- (3) Breen, J. J.; Kilogore, K.; Tzeng, W.-B.; Wei, S.; Keesee, R. G.; Castleman, A. W., Jr. *J. Chem. Phys.* **1989**, *90*, 11.
- (4) Stanley, R. J., Jr. *J. Chem. Phys.* **1990**, *92*, 5770.
- (5) Wana, J.; Meanapace, J. A.; Bernstein, E. R. *J. Chem. Phys.* **1986**, *85*, 1795.
- (6) Gonohe, N.; Abe, H.; Mikami, N.; Ito, M. *J. Phys. Chem.* **1985**, *89*, 3642.
- (7) The IR OPO was calibrated by measuring the wavelength of the red light ( $\sim$ 645 nm) generated by the sum frequency of signal and pump beams using a standardized monochromator. The absolute frequency calibration is within  $\pm 3 \text{ cm}^{-1}$ .
- (8) Frisch, M. J.; Trucks, G. W.; Schlegel, H. B.; Scuseria, G. E.; Robb, M. A.; Cheeseman, J. R.; Zakrzewski, V. G.; Montgomery, J. A., Jr.; Stratmann, R. E.; Burant, J. C.; Dapprich, S.; Millam, J. M.; Daniels, A. D.; Kudin, K. N.; Strain, M. C.; Farkas, O.; Tomasi, J.; Barone, V.; Cossi, M.; Cammi, R.; Mennucci, B.; Pomelli, C.; Adamo, C.; Clifford, S.; Ochterski, J.; Petersson, G. A.; Ayala, P. Y.; Cui, Q.; Morokuma, K.; Malick, D. K.; Rabuck, A. D.; Raghavachari, K.; Foresman, J. B.; Cioslowski, J.; Ortiz, J. V.; Stefanov, B. B.; Liu, G.; Liashenko, A.; Piskorz, P.; Komaromi, I.; Gomperts, R.; Martin, R. L.; Fox, D. J.; Keith, T.; Al-Laham, M. A.; Peng, C. Y.; Nanayakkara, A.; Gonzalez, C.; Challacombe, M.; Gill, P. M. W.; Johnson, B. G.; Chen, W.; Wong, M. W.; Andres, J. L.; Head-Gordon, M.; Replogle, E. S.; Pople, J. A. *Gaussian 03*, rev. B02; Gaussian, Inc.; Pittsburgh, PA, 2003.
- (9) Kim, S. K.; P; Tarakeshwar, P.; Lee, J. Y. *Chem. Rev.* **2000**, *100*, 4145.
- (10) (a) King, G. W.; So, S. P. *J. Mol. Spectrosc.* **1971**, *37*, 543. (b) Dao, P.-D.; Morgan, S., Jr. *J. Chem. Phys. Lett.* **1984**, *11*, 38.
- (11) (a) Iwasaki, A.; Fujii, A.; Ebata, T.; Mikami, N. *J. Phys. Chem.* **1996**, *100*, 16053. (b) Fujii, A.; Ebata, T.; Mikami, N. *J. Phys. Chem. A* **2002**, *106*, 8554.
- (12) Stearns, J. A.; Zwier, T. S. *J. Phys. Chem. A* **2003**, *107*, 10717.

(13) (a) Daunt, S. J.; Shurvell, H. F. *J. Mol. Spectrosc.* **1976**, *62*, 373.  
(b) Herzberg, G. *Infrared and Raman Spectra of Polyatomic Molecules*; Van Nostrand: New York, 1945.

(14) The deperturbation analysis was carried out for the 3325 and 3343  $\text{cm}^{-1}$  peaks following the recipe given in ref 14. It predicts the energy difference between the zero order vibrational states corresponding to the acetylenic C–H stretching vibration and the combination band of one quantum C $\equiv$ C stretch and two quanta of C $\equiv$ C–H out-of-plane bend to be 0.1  $\text{cm}^{-1}$ . This implies that the stretching frequency of the unperturbed acetylenic C–H group is 3334  $\text{cm}^{-1}$ .

(15) Pimentel, G. C.; McClellan, A. L. *The Hydrogen Bond*; Freeman: San Francisco, 1960.

(16) Singh, P. C.; Bandyopadhyay, B.; Patwari, G. N. *J. Phys. Chem. A* **2008**, *112*, 3360.

(17) Iwasaki, A.; Fujii, A.; Ebata, T.; Mikami, N. *J. Phys. Chem.* **1996**, *100*, 16053.

JP800064B